



STOCHASTIC DAMAGE ANALYSIS OF MASONRY STRUCTURES

Gianfranco LAEZZA¹, Alberto MANDARA² and Alessandra ZAMBRANO³

SUMMARY

The combined application of steel strengthening structures and dampers to up-grade masonry buildings is investigated in this paper. A viscous damping device and a steel bracing frame are added to a masonry panel in order to dissipate energy and provide additional strength. The optimization of the up-grading system is performed, in such way a damage-free performance under earthquake ground motion is achieved with a proper choice of viscous damper properties and frame stiffness. The influence of the uncertainties in the masonry strength on the optimal choice of the upgrading system is studied by means of a Monte Carlo simulation. Fragility curves for the unreinforced panel and for the upgraded panel with two types of retrofit solutions are evaluated, according to performance requirements set out by FEMA.

INTRODUCTION

Nowadays, an increasing interest in finding convenient and not invasive solutions for the seismic rehabilitation of existing masonry structures is shown by engineers and researchers. Innovative techniques, such as energy dissipation systems for the seismic retrofit of masonry structures, can be used as an alternative method to traditional solutions like cement and mortar injections or reinforced concrete sandwich panel jointed to masonry walls (Mandara [1],[2]). As a matter of fact, the use of passive energy control and dissipation techniques has been implemented in several projects for the seismic up-grading of existing buildings, including those with monumental and historical interest, as experienced in many applications carried out in recent years (Mazzolani [3], Indirli [4]).

In this context, an alternative approach consisting of connecting steel bracing to masonry structures by means of a viscous damper is proposed herein. This technique combines the advantages of steel frames (as lightness, stiffness, ductility, ease of assemblage and reversibility) to those of fluid viscous devices in order to allow a reduction of seismic impact by means of a great energy dissipation. The proposed combined system permits to achieve a twofold advantage: on one hand, a significant increase in stiffness, that improves the behavior of the masonry at the serviceability limit state; on the other hand, a remarkable energy dissipation, that enhances the structural response against seismic events of strong intensity, corresponding to the ultimate limit state. According to this approach, the request seismic performance can be reached by fitting the construction with adequate energy dissipation capability rather than by strengthening it with integrative structures. In such a way, not only an increase of the tolerable maximum

¹ Ph.D. Student, Seconda Università di Napoli. Department of Civil Engineering. Napoli, Italy.

² Professor, Seconda Università di Napoli. Dept. of Civil Eng. Napoli, Italy. Email:alberto.mandara@unina2.it

³ Researcher, Seconda Università di Napoli. Department of Civil Engineering. Napoli, Italy.

earthquake intensity can be achieved, but also a limitation of conventional strengthening interventions, which turns to be very useful when buildings have monumental features.

Generally speaking, the application of energy dissipation devices (EDD) requires the preliminary evaluation of their optimal properties and location. The most appropriate installation of dissipative devices can be chosen on the basis of a minimization of the predicted damage, by examining the possible collapse mechanisms. Proposed configurations of steel bracing elements and energy dissipation devices in masonry buildings are shown in Figure 1. In particular this type of retrofit system may be useful to protect long-bay masonry walls (Mazzolani [5]).

The best choice of the mechanical characteristic of both steel brace and energy dissipation system has been thoroughly investigated by Mazzolani [6], leading to some general conclusions on the most convenient range of brace-to-wall stiffness, strength ratios and optimal viscous constant to be adopted in practice.

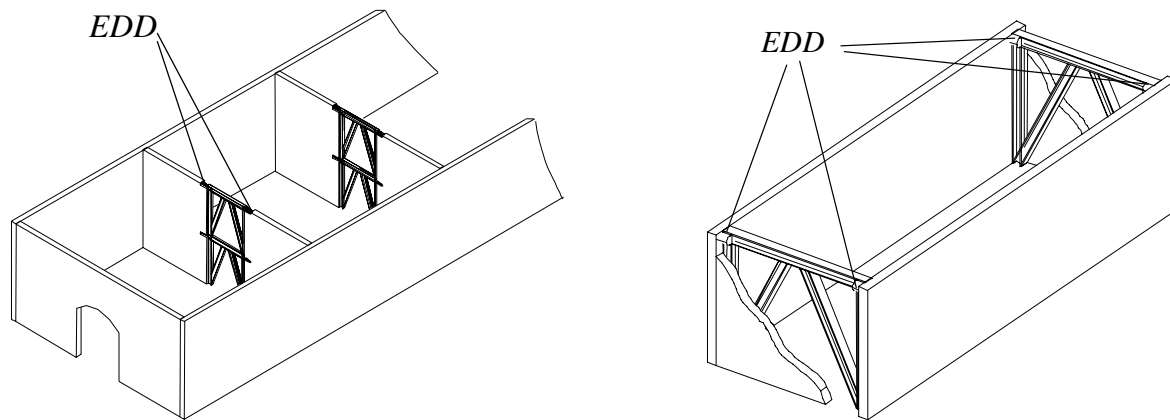


Figure 1. Examples of possible applications in masonry buildings.

The randomness of masonry properties for a given earthquake intensity level is taken into account herein, in order to evaluate its influence on the damage response of the masonry panel. To this purpose, two retrofitting solutions of combined bracing system and viscous damper are investigated. A Monte Carlo simulation, in which masonry strength is assumed as a random variable, has allowed to obtain fragility curves predicting the damage in the masonry panel, expressed in terms of maximum top displacement at increasing intensities of the ground motion. The results of this analysis have been interpreted in the light of “Performance Based Design”, according to requirements given in FEMA 356 Seismic Rehabilitation Prestandard [7].

In the first part of the paper, the adopted model of the masonry panel and steel bracing frame is presented. Then, the results of a parametric deterministic time-history analysis are summarized (Mazzolani [6]). In the successive paragraphs, the effectiveness of chosen retrofit systems is assessed and expressed through fragility curves.

MODELLING MASONRY PANEL AND BRACING FRAME

The study of this type of retrofit needs the definition of a model for both masonry panel and upgrading system. In the past, several studies have been performed to evaluate the mechanical characteristic and the seismic behavior of both masonry shear walls (Tomazevic [8]) and steel bracing structures (Engelhardt [9]), but the possibility to use a steel frame to upgrade a masonry panel has not received a particular interest till now. The proposed type of retrofit is shown in Figure 2. It consists of a panel upgraded with a steel eccentric braced frame connected by means of a linear viscous damper placed between the wall and

the bracing frame, so as to work for their relative displacements under seismic ground motions. This structural configuration has been analyzed by means of a time-history analysis assuming masonry panels with random variability of mechanical properties and increasing values of PGA. In the following the behavioral models adopted for both masonry panel and steel braced frame are discussed .

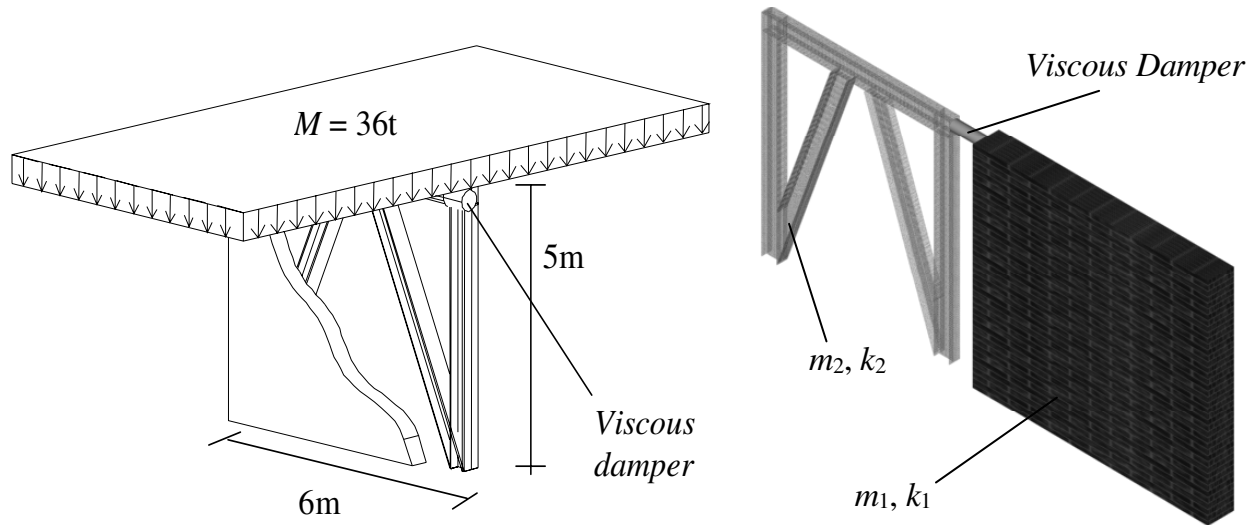


Figure 2. The model investigated in the analysis and its plane schematization.

The masonry panel model

Although the masonry is the most ancient material used in constructions, a general analytical model describing its behavior under horizontal loads is difficult to define, due to the difficulty in modeling the inelastic, not homogeneous and anisotropic behavior of material. In addition, uncertainties in material properties, especially in the case of unreinforced masonry, may lead to inaccurate evaluation of the seismic response, as well as of the corresponding safety level.

A considerable number of experiments to simulate the seismic behavior of masonry has been performed in the last decade, confirming that the shear behavior of unreinforced masonry is remarkably brittle, in particular for relatively low values of acting compressive stress. Nevertheless, when ultimate deformation limits are not exceeded, masonry shear panels do offer hysteretic behavior and, hence, energy dissipation capabilities. Stiffness and strength degradation, however, occurs when the panel is deeply stressed in plastic range, and this may substantially influence the interaction with the steel frame.

In order to have an accurate insight into such interaction, a refined non-linear model has been used for both masonry and steel structure. To this purpose, the advanced non-linear dynamic code CANNY has been used for the time-history analysis of the panel system (Li [10]). The global behavior of masonry panel under cyclic actions has been described by means of a trilinear shear-displacement model. The corresponding skeleton curve and mechanical characteristics are shown in Figure 3.

In order to consider the effect of the vertical load on the shear resistance of the masonry, the panel has been modelled through five horizontal layers, each of which has been characterized by a proper value of ultimate shear resistance as proposed by Turnsek e Cacovic and also introduced in the Italian code.

The panel model is characterized by stiffness and strength degradation, as well as by pinching behavior. Seven parameters are used in such a model to take into account the unloading stiffness (δ , θ), the strength deterioration (λ_e , λ_w , λ_3) and the pinching behavior (ε , λ_s) of the masonry with a good degree of accuracy. The meaning of the investigated parameters is illustrated in the following.

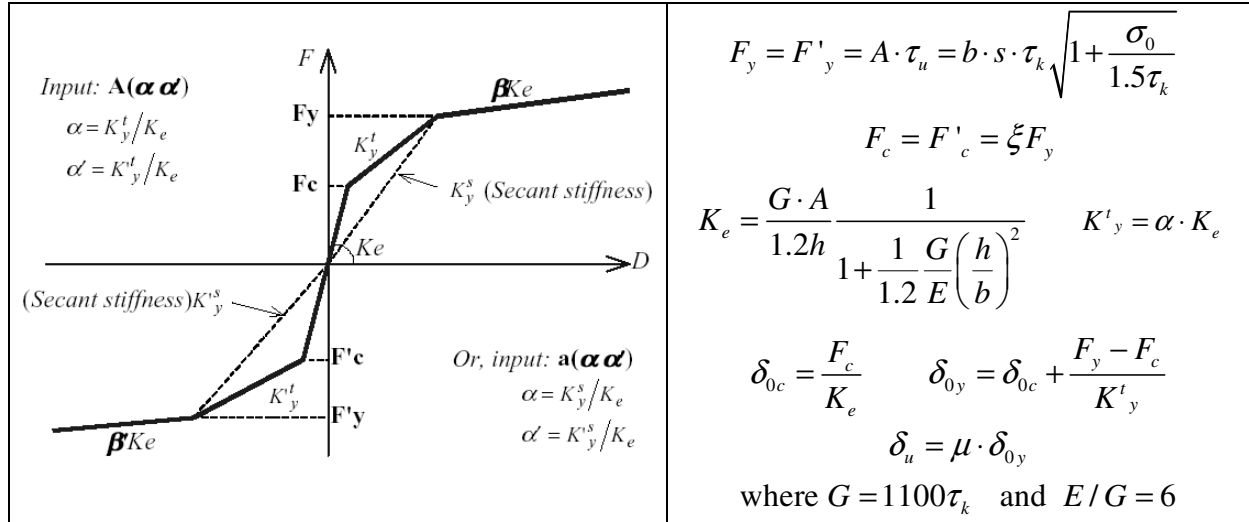


Figure 3. The skeleton curve of masonry panel model and its relevant mechanical characteristics.

Stiffness degradation

The unloading curve following a new peak displacement is directed to a target point E (or E') depending on the parameter θ , as shown in Figure 4a. The instantaneous stiffness of unloading branches is given by:

$$K_U = \frac{\theta F_y + F_m}{\theta F_y / K_0 + d_m}$$

The unloading branch from an outside loop ends at an sloped axis UU', whose gradient axis is equal to δK_0 , where K_0 is stiffness at the previous loop.

Strength deterioration

The model can reproduce the strength deterioration by directing the reloading curve towards a reduced strength level \bar{F}_{\max} at the same displacement corresponding to the previous peak strength F_{\max} , as shown in Figure 4b. \bar{F}_{\max} is evaluated considering the attained ductility and the dissipated hysteresis energy according the following relationship:

$$\bar{F}_{\max} = F_{\max} \left(1 - \lambda_e \frac{E_h}{F_y d_{\max} + F'_y d'_{\max}} - \lambda_u \left(1 - \frac{1}{\mu} \right) \right)$$

The softening effect is represented by a third parameter λ_3 that lowers the post-yield envelope:

$$\bar{K}_{py} = K_{py} \left(1 - \lambda_3 \left(1 - \frac{1}{\mu} \right) \right) \quad \text{with} \quad \bar{K}_{py} \geq 0.01 K_{py}$$

Pinching behaviour

The pinching behaviour simulates the opening and closing of cracks. Target point (F_e, d_e) controls the slip branches, as shown in Figure 4c.

$$\begin{cases} d_e = \varepsilon d_u \\ F_e = \lambda_s \left(\bar{F}_{\max} - \delta \cdot K_0 \cdot d_{\max} \right) + \delta \cdot K_0 \cdot d_{\max} \end{cases}$$

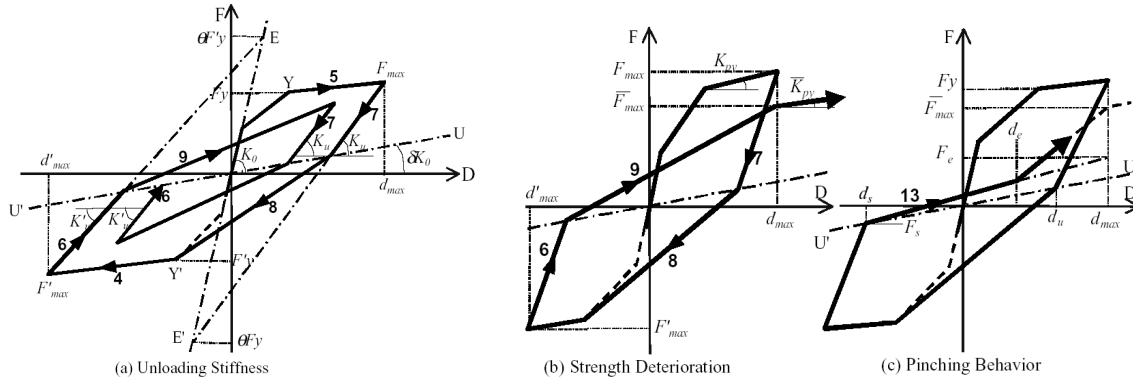


Figure 4. The cycling behaviour of the masonry model.

The braced frame model

The mechanical behavior of steel bracing has been interpreted by means of the Canny BL2 model, showing an elastic-plastic relationship which closely reproduces the stable hysteretic response of eccentric braced frame as shown in Figure 5. This feature is typical of eccentric bracing systems characterized by short shear link, that is an element yielding predominately in shear. Model BL2 has a bilinear skeleton curve. It forms equal-degrading unloading stiffness in both positive and negative sides. The reloading curve follows the unloading without stiffness change and a new yielding may occur before the displacement changes sign. The model is characterized by a unique parameter γ , which rules the slope of the unloading curve:

$$K_u = K_0 \left(\frac{d_y - d'_y}{d_m - d'_m} \right)^\gamma$$

In the present analysis, according to the results of numerous tests referred in literature, no stiffness degradation has been considered, which corresponds to $\gamma=0$.

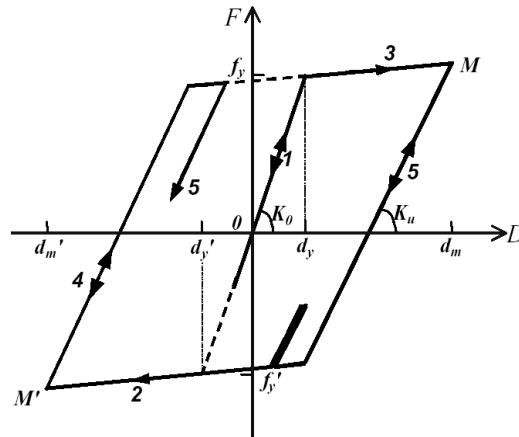


Figure 5. The steel bracing model.

EVALUATION OF OPTIMAL SYSTEM PROPERTIES

The combined application of steel strengthening structures and passive control techniques to masonry buildings has been extensively investigated in a previous research (Mazzolani [6]). A comprehensive numerical analysis of the above mentioned system has been carried out, in which the optimal properties of

the protection elements have been evaluated by means of time-history response analysis. System optimization has been performed by minimizing the response in terms of top panel displacement. To this aim, a purposely conceived damage index, named Deformation Damage Index (*DDI*), has been introduced, defined as:

$$DDI = \frac{\delta - \delta_{\min}}{\delta_u - \delta_{\min}}$$

with the following meaning of the symbols:

- δ maximum in-plane top displacement of the panel across the entire earthquake time-history;
- δ_{\min} maximum in-plane top displacement value for optimal viscous properties;
- δ_u ultimate in-plane displacement of the wall;

Because of its inherent definition *DDI* can also result greater than unity, which means that collapse has been attained. The no-damage threshold is set when $\delta = \delta_e$, where δ_e is the displacement at the elastic limit.

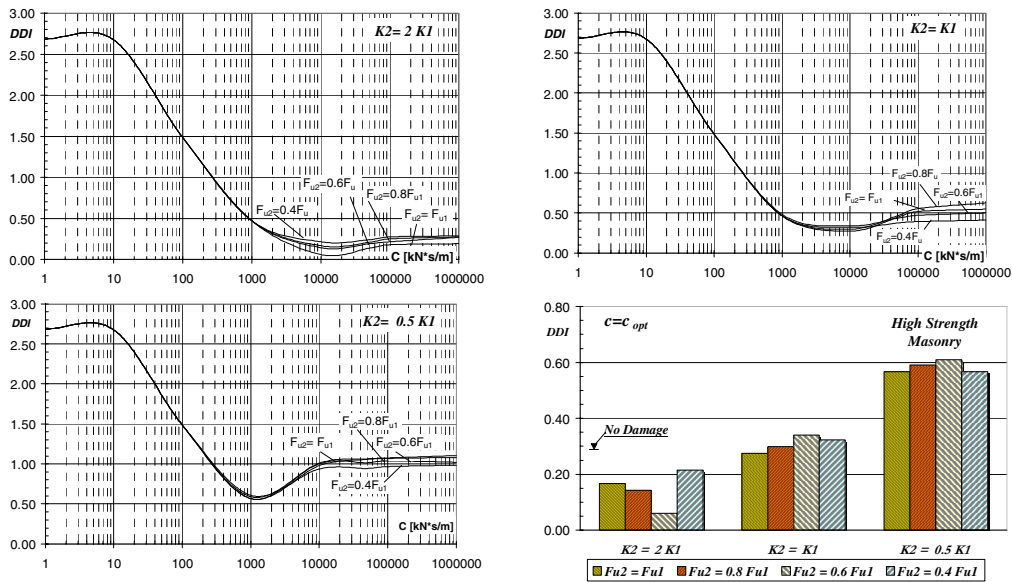


Figure 6. Values of DDI as a function of viscous constant *c* (Calitri earthquake).

Panels with different material properties have been studied in the time domain for a number of earthquake recordings, scaled to a PGA equal to 0.40g. Results of the analysis put into evidence the influence of device viscous constant *c* on the global structural behavior. In particular, within an optimal range of the device viscous constant, the use of viscous devices strongly reduces the structural response in terms of both shear force and displacement. Results for a panel made of the high-strength masonry, whose properties are shown in Table 1, are presented herein. The panel geometry and parameters are reported in Table 2. Symbol notation is explained in Figure 3. The complete absence of damage is achieved when the steel bracing stiffness k_2 is higher than the in-plane panel stiffness k_1 , namely when $k_2 \geq (1+2)k_1$. Defining F_{u2} and F_{u1} as the ultimate shear force of steel bracing system and masonry panel respectively, the structural response is not so strongly dependent on the F_{u2}/F_{u1} ratio as long as $F_{u2}/F_{u1} > 0.5$. Figures 6 to 8 show the damage response of the masonry panel under three seismic inputs, namely Calitri (1980), El Centro (1940) and Taiwan (1999). They also emphasize the influence of device viscous constant *c* on the value of the Damage Deformation Index. The value c_{opt} that minimizes *DDI* when $k_2 \geq (1+2)k_1$ is around 10000 kNs/m and is, as expected, rather independent of the seismic input. Histograms in Figures 6 to 8 show the influence of both stiffness and strength ratios on the structural response.

Table 1. Material properties of the considered masonry.

τ_k	σ_k	G	E
[N/mm ²]	[N/mm ²]	[N/mm ²]	[N/mm ²]
0.1	2.5	110	660

Table 2. Panel model characteristics.

Height h [m]	Length [m]	Width [m]	δ_{δ_c} [mm]	δ_{δ_y} [mm]	δ_u [mm]	ξ	α	μ
5.00	6.00	0.40	7.08	8.64	20.75	0.85	0.8	2.5

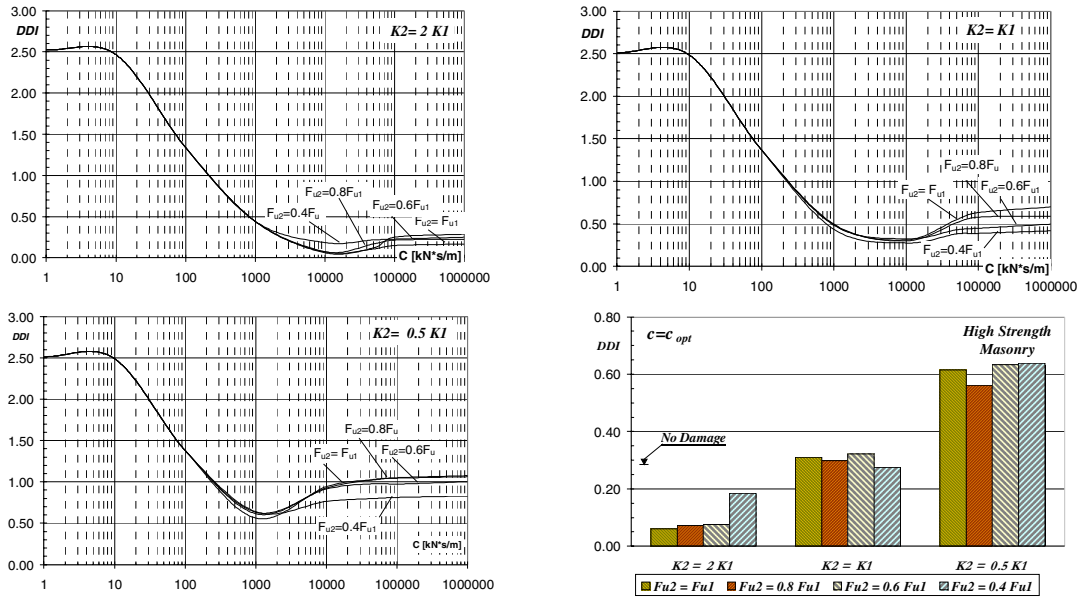


Figure 7. Values of DDI as a function of viscous constant c (El Centro earthquake).

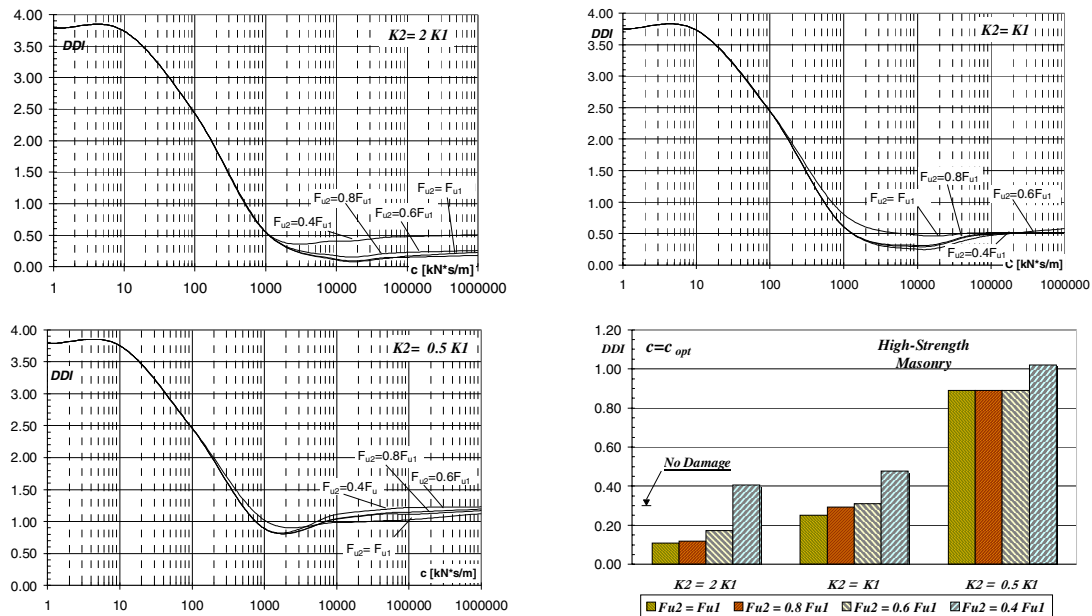


Figure 8. Values of DDI as a function of viscous constant c (Taiwan earthquake).

STOCHASTIC RESPONSE ANALYSIS

Procedure description

The variability in the response of the masonry structures to earthquake ground motions depends on many sources of randomness: material properties, vertical loads, seismic events, structural geometry, material quality and assemblage. These uncertainties should be taken into account when a retrofit design is undertaken. A poor knowledge of suitable design values of above magnitudes, in fact, can impair the effectiveness of the adopted upgrading solution. In particular, the evaluation of the seismic response of masonry structures by means of a deterministic analysis could lead to an unsatisfactory agreement between predicted and surveyed damage. A possible way to account for the inherent property variability is to assess the seismic response of the system by performing a stochastic analysis considering the random nature of panel strength.

The use of fragility curves providing the probability of occurrence of a pre-defined limit state for a given PGA is proposed to assess the effectiveness of the upgrading system (Shinozuka [11]). The probabilistic analysis is developed by means of the Monte Carlo method (Rubinstein [12]), which consists of analyzing the response of nominally identical panels, but structurally different in terms of shear strength τ_k , which is generated randomly. The panel sample is successively investigated via nonlinear time-history dynamic analyses. In the end, the seismic reliability of the structure is determined by means of fragility curves.

The panel response has been quantified by means of the maximum top displacement δ normalized to the panel height h , so as a ‘‘Top Displacement Angle’’ (*TDA*) is defined:

$$TDA = \frac{\delta}{h}$$

The structural response is then evaluated according to the ‘‘Performance Based Design’’. As prescribed in FEMA 356 [7], three performance levels have been considered: Immediate Occupancy (I.O.), Life Safety (L.S.), Collapse Prevention (C.P.), corresponding to the predetermined values of *TDA* listed in Table 3.

Table 3. Acceptance criteria of TDA for primary masonry walls according to FEMA356.

	Performance level		
	Immediate occupancy (I.O.)	Life safety (L.S.)	Collapse prevention (C.P.)
Bed-joint sliding	0.001	0.003	0.004
Rocking	0.001	$0.003h_{\text{eff}}/L$ (*)	$0.004h_{\text{eff}}/L$ (*)

(*) h_{eff} and L are the wall effective height and length, respectively.

The seismic event is another principal source of randomness in the response. In fact, basic seismic hazard at a site, phasing, amplitude and frequency content are random. To accomplish the task to evaluate the probability of occurrence to attain a given limit state under earthquakes, simulated ground motions generated to match Eurocode 8 soil type B spectra have been considered, with a PGA ranging between $0.05g$ and $0.70g$.

The Cumulative Density Function (CDF), namely $F(x)$, for a given PGA is defined as:

$$F[x_i | \text{PGA}] = P[x < x_i | \text{PGA}]$$

The fragility of a structure $F_f(x)$ is defined as its probability to attain a given limit-state, conditioned on a specific PGA, that is consistent with the specific seismic hazard:

$$F_f[x_L | \text{PGA}] = P[x \geq x_L | \text{PGA}] = 1 - P[x < x_L | \text{PGA}] = 1 - F[x_L | \text{PGA}]$$

where x_L means the corresponding limit-state. $F_f(x)$ is modeled with a log-normal distribution, this assumption has been confirmed by the statistical cumulative values evaluated on the basis the Monte Carlo simulation results.

The fragility curve according to FEMA limit states is obtained for the corresponding value of TDA . For instance, considering as limit state the performance level related to $x_L = TDA_L = 0.001$ (Immediate Occupancy level), the corresponding fragility function at a given PGA is:

$$F_f[0.001|PGA] = P[TDA \geq 0.001|PGA] = 1 - P[TDA < 0.001|PGA]$$

The fragility curves in terms of TDA corresponding to the three performance levels (Immediate Occupancy, Life Safety and Collapse Prevention) are evaluated according to the Monte Carlo numerical procedure described as follows:

1. *Random generation of the panel strength.* Different panels with identical geometry are considered (see Table 2), in which τ_k has been generated randomly with a normal distribution having a mean of 0.1N/mm^2 and a standard deviation of 0.03N/mm^2 , an average in-plane panel stiffness equal to $k_1=30000\text{ kN/m}$ corresponds to this mean value;
2. *Generation of the earthquake recordings*, compatible with Eurocode 8 for soil B;
3. *Scaling of the seismic recordings to different excitation level*;
4. *Seismic analysis.* The generated panels are investigated via non linear dynamic analysis in order to obtain a statistical sample of the inelastic seismic response;
5. *Statistical interpretation of the results*, which consists of:
 - Selection of the control variable $x = TDA$ to evaluate the seismic structural response;
 - Rank-ordering of the control variable obtained from nonlinear dynamic analyses ($x_1 \leq x_2 \leq \dots \leq x_{n-1} \leq x_n$ where n is the sample size, i.e. the number of analyzed panels);
 - Determination of statistical CDF values corresponding to the i -th value (x_i) of the control variable;
 - Estimation of the mean value and standard deviation of the rank-ordered series, plotting the number of occurrences of each x_i at each excitation level on a lognormal probability graph and execution of a linear regression analysis;
 - Calculation of the log-normal cumulative probability for any PGA;
 - Evaluation of cumulative probability for any fixed limit value of the control variable (x_i) for given PGA values;
 - Determination of the fragility curves for x_L values corresponding to FEMA performance levels for given value of PGA:

$$F_f(x_L) = P[x \geq x_L | PGA]$$

6. *Plotting of the (PGA, $F_f(x_L)$) values* on the log-normal probability graph and regression analysis to obtain the fragility curve;
7. *Representation of the fragility curve*, assuming a log-normal distribution corresponding to each performance level.

Results of Monte Carlo simulation

The mean value and the standard deviation of TDA are reported in Figures 9 and 10 as a function of PGA for cases: a) the unreinforced panel; b) the retrofitted panel with a viscous damper having $c = c_{\text{opt}} = 10000\text{ kNs/m}$ and a frame with stiffness $k_2 = 30000\text{ kN/m}$ (retrofit type 1); c) the retrofitted panel with a viscous damper having a $c = 5000\text{ kNs/m}$ and a frame stiffness $k_2 = 15000\text{ kN/m}$ (retrofit type 2). Retrofit options differ in the choice of both viscous constant c and frame stiffness k_2 , so to assess the influence of masonry strength randomness on the main system parameters. In particular, the influence of system parameters other than the optimal ones has been investigated, in order to evaluate their effect on the global structural performance. In this view, assuming type 2 retrofit option would mean to adopt a protection system with reduced properties and, hence, with lower cost compared with option 1.

Looking at results, the *TDA* mean value (Figure 9) shows the effectiveness of the two types of retrofit compared with the unreinforced panel. In average, type 1 retrofit gives the lowest values of *TDA* with a very little data scattering (Figure 10). Nevertheless, option 2 provides results very similar to those given by option 1 and both solutions lead to a significant reduction of *TDA*, i.e. of top panel displacement, compared with plain masonry wall. In Figures 11 to 13, showing the CDF of the three systems for six different levels of PGA, the difference between the two protection options is more evident, and shows the higher reliability of option 1. This is clear also from Figures 14 to 16, where the curves, for the assigned performance levels, can be used to determine both the fragility corresponding to a given PGA and, conversely, the maximum PGA that the structure is able to sustain with a certain probability without overcome the limit value corresponding to the considered performance level. Figures 17 to 19 report in the form of histogram the CDF $F[TDA|PGA]$ corresponding to the three FEMA performance levels for the three systems. Figures 20, in the end, shows the *TDA* limit values corresponding to a 50% attainment probability as a function of PGA for the three considered retrofit options. Figures 17 to 20 confirm the relatively small difference between the reliability levels offered by the two protection options. Generally speaking, the good performance of both systems is clearly evident, since the Collapse Prevention level is never overcome until the PGA is not greater than 0.55g and 0.40g for option 1 and 2, respectively. In terms of maximum tolerable PGA, this causes that, for a PGA = 0.7g, the probability to avoid collapse ($TDA < 0.004$, C.P. performance level), is still equal to 58% for option 1 and 22% for option 2. From fragility curves (Figures 14 to 16) and related histograms (Figures 17 to 19) it is also possible to observe that the application of both protection systems greatly widens the serviceability range of the wall, in the sense that the wall is prevented from any damage up to PGA equal to about 0.2g and 0.05g for option 1 and option 2, respectively, whereas in the same conditions the performance of the unprotected systems is much lower. In particular, the performance improvement obtained when adopting option 1 mostly lays in its higher protection against the I.O. and L.S. performance levels. On the contrary, concerning the C.P. performance level, the advantage in using option 1 instead of option 2 is comparatively smaller.

All the above considerations would seem to confirm the effectiveness of the proposed solution also for system values different from optimal ones. In particular, the randomness of masonry strength values would tend to make less critical the choice of systems parameters and this involves the possibility to adopt cheaper and/or simplified protection systems, with tangible benefits mainly when operating on historical and monumental buildings. From the analysis carried out herein, in fact, also comparatively lower values of both viscous constant and frame stiffness (option 2) lead to satisfying improvements of structural performance under seismic action, in particular when the ultimate limit state (C.P.) is considered.

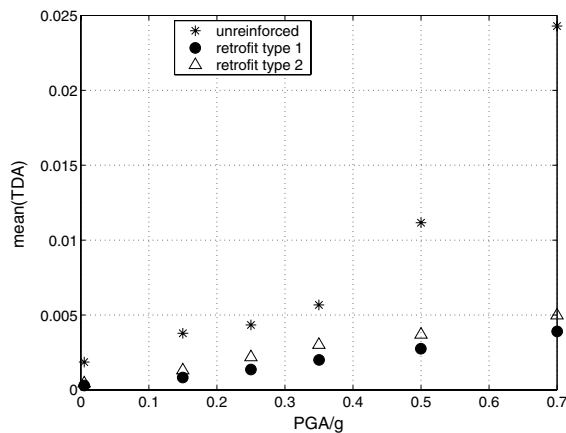


Figure 9. Mean Value of *TDA*.

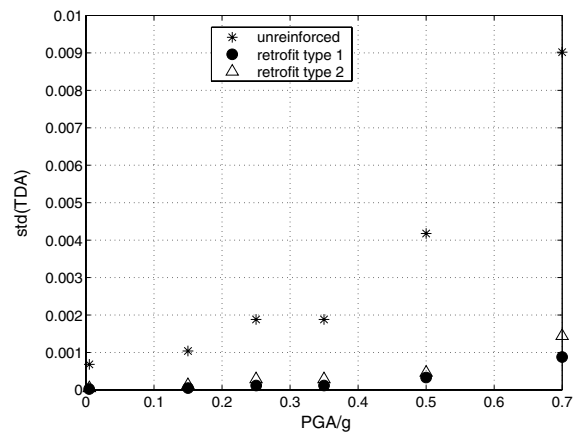


Figure 10. Standard Deviation of *TDA*.

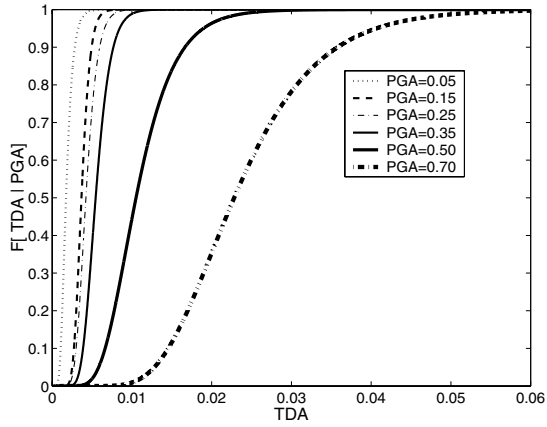


Figure 11. CDF of *TDA* for a given PGA of the unreinforced panel.

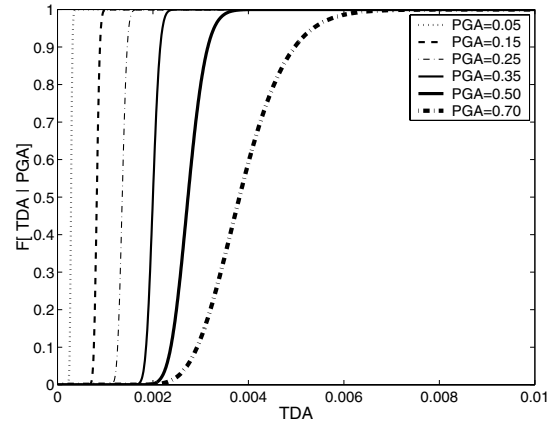


Figure 12. CDF of *TDA* for a given PGA of the panel with retrofit type 1.

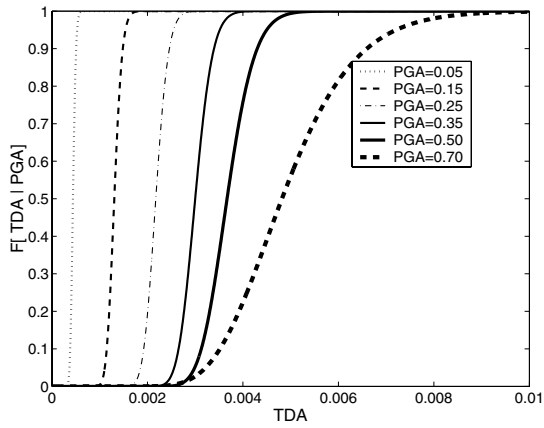


Figure 13. CDF of *TDA* for a given PGA of the panel with retrofit type 2.

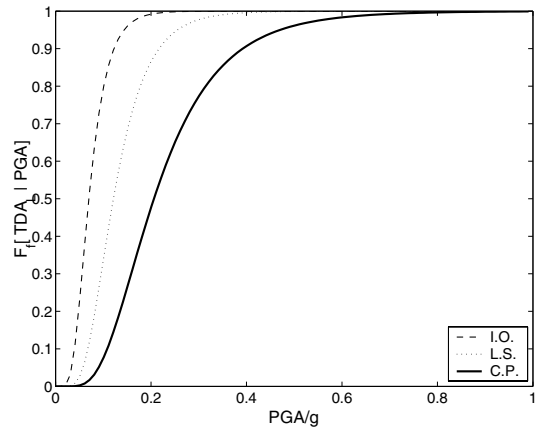


Figure 14. Fragility curves in terms of *TDA* for the unreinforced panel.

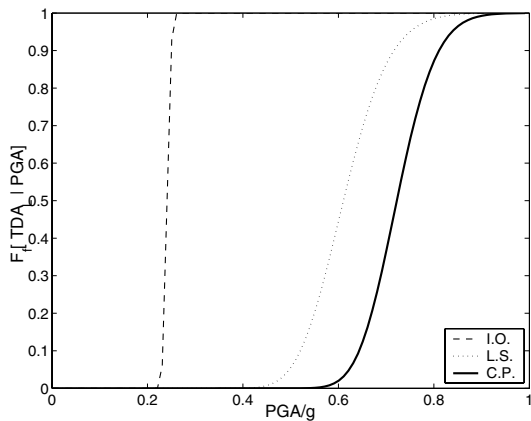


Figure 15. Fragility curves in terms of *TDA* for the retrofitted panel (type 1).

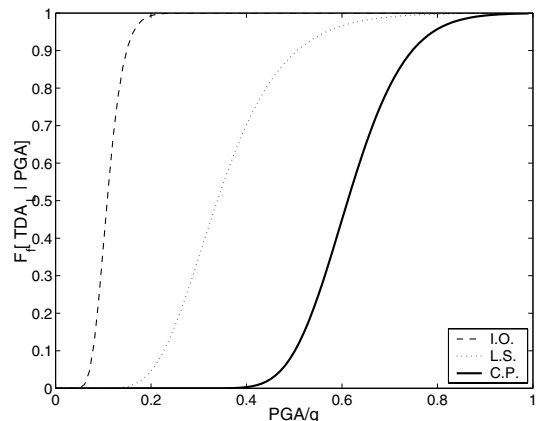


Figure 16. Fragility curves in terms of *TDA* for the retrofitted panel (type 2).

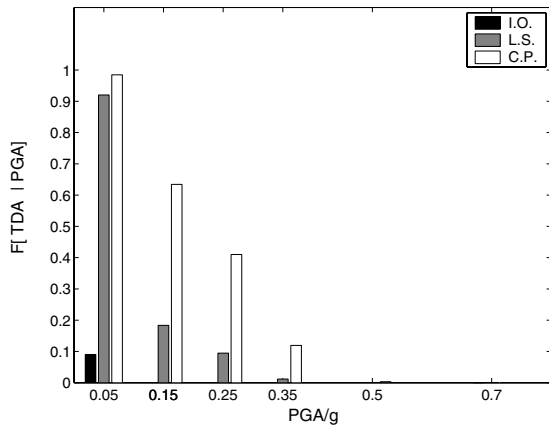


Figure 17. CDF of the unreinforced panel at different performance levels according to FEMA 356.

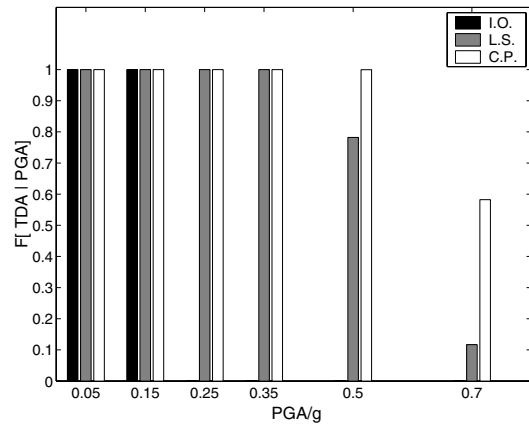


Figure 18. CDF of the retrofitted panel at different performance levels according to FEMA 356 (type 1).

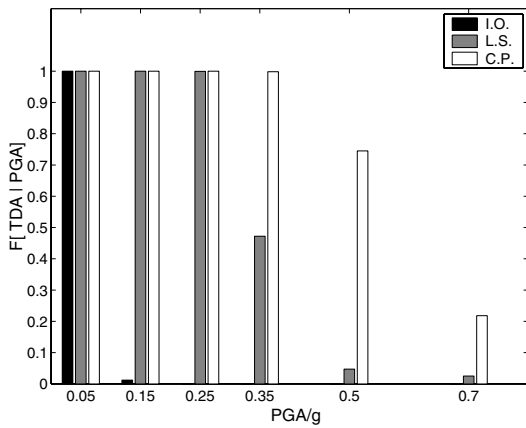


Figure 19. CDF of the retrofitted panel at different performance levels according to FEMA 356 (type 2).

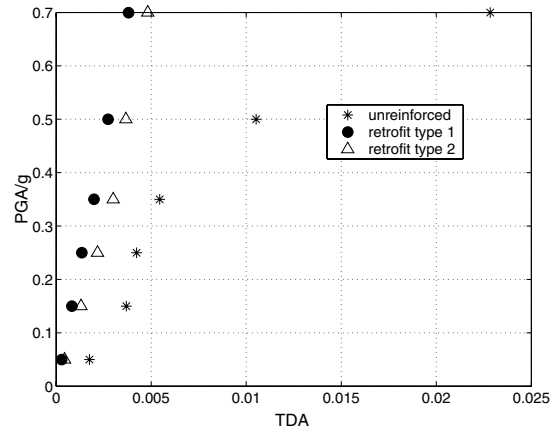


Figure 20. PGA versus maximum TDA corresponding to a $F[TDA|PGA] = 0.5$.

CONCLUSIONS

The possibility of upgrading masonry structures through steel structures and energy dissipation devices has been analyzed in this paper. An extensively deterministic parametric analysis carried out on a masonry wall connected to a steel braced frame by means of a viscous damping device has preliminarily allowed to evaluate the system properties which minimized the structural response under seismic actions. Afterwards, the effectiveness of the optimum solutions has been assessed through a stochastic analysis in which the strength of the masonry has been assumed to have a random distribution. A procedure based on the Monte Carlo simulation, aiming at the evaluation of the fragility curves corresponding to predefined performance levels, has been illustrated taking into account two different protection options. The exam of results shows that a good effectiveness of the proposed solution is possible also for system values different from optimal ones. In particular, under certain circumstances, the randomness of masonry strength may lead to adopt cheaper and/or simplified seismic protection solutions, which turns to be useful in case of retrofit of historical constructions, without significant reductions of structural performance.

ACKNOWLEDGEMENTS

This work has been developed within the research project entitled “Integrative metal-based systems for the seismic up-grading of existing buildings” (responsible A. Mandara), which is a part of the national research project “Innovative metal-based structures for seismic retrofitting of new and existing buildings: criteria and design methodologies ”(PRIN-2003), issued by the Italian Ministry of University and Research (MIUR) and coordinated by F.M. Mazzolani.

REFERENCES

1. Mandara A., Mazzolani F.M., “On the Design of Retrofitting by means of Energy Dissipation Devices”, Proceedings of 7th International Seminar on Seismic Isolation, Passive Energy Dissipation and Active Control of Vibrations of Structures, Assisi, Italy, 2001.
2. Mandara A., Mazzolani F.M., “Energy Dissipation Devices in Seismic Up-Grading of Monumental Buildings”, Proc. of III Seminar on Historical Constructions, Guimaraes, Portugal, 2001.
3. Mazzolani F.M., Mandara A., “Seismic Upgrading of Churches by Means of Dissipative Devices”, In F.M. Mazzolani & V. Gioncu (eds), Behaviour of Steel Structures in Seismic Areas STESSA '94. E & FN SPON, London, p. 747-758, 1994.
4. Indirli M., “The Demo-Intervention of the ISTECH Project: the Bell Tower of S. Giorgio in Trignano (Italy)”, Proc. of the Final Workshop of ISTECH Project, Ispra (Italy), p. 141-153, 2000.
5. Mazzolani F.M., Mandara A., Froncillo S., “Dissipative steel structures for seismic up-grading of long-bay masonry buildings”, In F.M. Mazzolani (ed.), Behaviour of Steel Structures in Seismic Areas STESSA 2003, Balkema, Amsterdam, 2003.
6. Mazzolani F.M., Mandara A., Froncillo S., Laezza G., “Design criteria for the use of special devices in the seismic protection of masonry structures”, 8th World Seminar on Seismic Isolation, Energy Dissipation and Active Vibration Control of Structures Yerevan, Armenia, October 6-10, 2003.
7. FEMA 356 “Prestandard and Commentary for the Seismic Rehabilitation of Buildings”, Report by the American Society of Civil Engineering (ASCE) for the Federal Emergency Management Agency (FEMA), Washington, D.C, 2000.
8. Tomazevic M., Lutman M., “Seismic behavior of masonry walls: modeling of hysteretic rules”, Journal of Structural Engineering, 122, 9, pp.1048-1054, 1996.
9. Engelhardt M.D., Popov E.P., “On Design of Eccentrically Braced Frames”, Earthquake Spectra, Vol. 5, No. 3, 1989.
10. Li K., “3-dimensional nonlinear static/dynamic structural analysis computer program - CANNY 99 “ - Technical Manual, 1996.
11. Shinozuka, M., “Basic Analysis of Structural Safety”, Journal of Structural Engineering, ASCE, vol.109 (3) pp.721-740, 1983.
12. Rubinstein R.Y., “Simulation and the Monte Carlo Method”, John Wiley & Son, 1992.